

A SEARCH FOR ACTIVE GALACTIC NUCLEI IN SC GALAXIES WITH H II SPECTRA

JAMES S. ULVESTAD

National Radio Astronomy Observatory¹, P.O. Box O, Socorro, NM 87801
julvesta@nrao.edu

AND

LUIS C. HO

The Observatories of the Carnegie Institution of Washington, 813 Santa Barbara St., Pasadena, CA 91011
lho@ociw.edu*To appear in The Astrophysical Journal.*

ABSTRACT

We have searched for nuclear radio emission from a statistically complete sample of 40 Sc galaxies within 30 Mpc that are optically classified as star-forming objects, in order to determine whether weak active galactic nuclei might be present. Only three nuclear radio sources were detected, in NGC 864, NGC 4123, and NGC 4535. These galaxies have peak 6-cm radio powers of $\sim 10^{20}$ W Hz⁻¹ at arcsecond resolution, while upper limits of the non-detected galaxies typically range from $10^{18.4}$ W Hz⁻¹ to 10^{20} W Hz⁻¹. The three nuclear radio sources all are resolved and appear to have diffuse morphologies, with linear sizes of ~ 300 pc. This strongly indicates that circumnuclear star formation has been detected in these three H II galaxies. Comparison with previous 20-cm VLA results for the detected galaxies shows that the extended nuclear radio emission has a flat spectrum in two objects, and almost certainly is generated by thermal emission from gas ionized by young stars in the centers of those galaxies. The 6-cm radio powers are comparable to predictions for thermal emission that are based on the nuclear H α luminosities, and imply nuclear star formation rates of $0.08 - 0.8 M_{\odot} \text{ yr}^{-1}$, while the low-resolution NRAO VLA Sky Survey implies galaxy-wide star formation rates of $0.3 - 1.0 M_{\odot} \text{ yr}^{-1}$ in stars above $5 M_{\odot}$. In a few of the undetected galaxies, the upper limits to the radio power are lower than predicted from the H α luminosity, possibly due to over-resolution of central star-forming regions. Although the presence of active nuclei powered by massive black holes cannot be definitively ruled out, the present results suggest that they are likely to be rare in these late-type galaxies with H II spectra.

Subject headings: galaxies: active — galaxies: nuclei — galaxies: Seyfert — galaxies: starburst — radio continuum: galaxies

1. INTRODUCTION

Most nearby normal and active galaxies with bulges appear to have supermassive black holes at their centers (see Kormendy & Gebhardt 2001 for a review), and the masses of these black holes ($\sim 10^6 M_{\odot} - 10^9 M_{\odot}$) seem well correlated with the galaxy bulge masses as inferred from the bulge luminosities (Magorrian et al. 1998). In fact, the relation of black hole mass to bulge stellar velocity dispersion is a correlation with far less scatter than that derived from the bulge luminosity (Ferrarese & Merritt 2000; Gebhardt et al. 2000a; Tremaine et al. 2002). The black hole masses from this relation are consistent with those derived from the widths of broad emission lines and their distances from the black hole as derived by reverberation mapping (Gebhardt et al. 2000b; Ferrarese et al. 2001). The relation of black hole mass to bulge mass appears confirmed in at least one bulgeless galaxy, the nearby spiral M33, where an upper limit of $1500 - 3000 M_{\odot}$ has been found for the black hole mass (Gebhardt et al. 2001; Merritt, Ferrarese, & Joseph 2001).

Ho, Filippenko, & Sargent (1995, 1997a, 1997b) used the Palomar 200 inch telescope to perform a spectroscopic survey of 486 bright, nearby galaxies selected from the Revised Shapley-Ames Catalog of Bright Galaxies (Sandage & Tammann 1981), in order to conduct a census of the population of active galactic nuclei (AGNs) in the nearby universe. Fifty-two Seyfert galaxies were found in that survey, and 82% of the

objects in a statistical sample of 45 of these Seyferts were detected using the Very Large Array (VLA) at 6 cm, with observations of 15–18 min in length (Ho & Ulvestad 2001; Ulvestad & Ho 2001). The detected radio sources in these low-luminosity Seyferts typically are associated with the AGNs, implying the presence of massive black holes powering the active nuclei.

In addition to the 52 Seyferts identified by Ho et al. (1997a), 206 galaxies from the Palomar sample were reported to contain H II nuclei: galaxy nuclei with optical line ratios consistent with ionization by young, massive stars. As a general (though not universal) rule, the AGNs (Seyferts and LINERs) are found in early-type galaxies (earlier than Sbc), while the H II nuclei are found in galaxies of type Sb or later.

Although the late-type galaxies in the Palomar sample that are classified as H II galaxies appear to be dominated by star formation, it also is possible that they contain weak AGNs whose optical signature has simply been overpowered by the more dominant signal from nuclear H II regions. The presence of an AGN typically requires two constituents: a massive central black hole and a supply of gas to “feed” that black hole. Since galaxies with H II spectra generally harbor copious supplies of gas, the question of whether H II-dominated objects contain observable AGNs then may be equivalent to the question of whether these galaxies contain massive central black holes. Good discriminators for the presence of an AGN include the presence of a compact source of hard X-rays or radio

¹ The National Radio Astronomy Observatory is a facility of the National Science Foundation, operated under cooperative agreement by Associated Universities, Inc.

TABLE 1
VLA OBSERVATIONS OF H II GALAXIES

(1) Galaxy	(2) Date	(3) Array	(4) Integration (min)	(5) α (J2000) ^a (h m s)	(6) δ (J2000) ^a ($^{\circ}$ ' ")	(7) Distance ^b (Mpc)	(8) rms (μ Jy beam ⁻¹)
NGC 864 ^c	1985–1991	B	35	02 15 27.63	+06 00 08.5	20.0	49
NGC 1073 ^c	1985–1991	B,A	37	02 43 41.81	+01 22 58.4	15.2	83
IC 467	2000Oct16	A	3.5	07 30 17.30	+79 52 21.0	31.7	100
NGC 2715	1987Nov06	BnA	22	09 08 07.13	+78 05 21.2	20.4	58
NGC 2742	2000Oct16	A	3.5	09 07 33.20	+60 28 46.0	22.2	100
NGC 2770	2000Oct16	A	3.5	09 09 33.41	+33 07 40.4	29.6	100
NGC 2976	1989–1991	B	33	09 47 15.60	+67 54 49.5	2.1	47
NGC 3041	2000Oct16	A	3.5	09 53 07.20	+16 40 40.0	22.8	100
NGC 3198	2000Oct16	A	3.5	10 19 54.90	+45 32 58.8	10.8	100
NGC 3294	1991Jun15	A	8	10 36 16.11	+37 19 20.1	26.7	68
NGC 3338	2000Oct16	A	3.5	10 42 07.50	+13 44 49.0	22.8	100
NGC 3359 ^c	1985–1991	B,BnA	144	10 46 36.52	+63 13 17.6	19.2	38
NGC 3370	2000Oct16	A	3.5	10 47 03.78	+17 16 26.5	23.4	100
NGC 3389	2000Oct16	A	3.5	10 48 27.89	+12 32 00.0	22.5	100
NGC 3596	2000Oct16	A	3.5	11 15 06.29	+14 47 12.1	23.0	100
NGC 3631	2000Oct16	A	3.5	11 21 02.90	+53 10 10.0	21.6	100
NGC 3655	2000Oct16	A	3.5	11 22 54.57	+16 35 23.8	26.5	100
NGC 3666	1984Dec08	A	4.5	11 24 26.20	+11 20 31.0	17.0	130
NGC 3726	2000Oct16	A	3.5	11 33 20.73	+47 01 40.5	17.0	100
NGC 3810	2000Oct16	A	3.5	11 40 58.80	+11 28 16.7	16.9	100
NGC 3877 ^c	1999Oct28	B	15	11 46 06.13	+47 28 55.4	17.0	70
NGC 3893	2000Oct16	A	3.5	11 48 38.04	+48 42 40.1	17.0	100
NGC 3938	2000Oct16	A	3.5	11 52 49.55	+44 07 13.7	17.0	100
NGC 4062	2000Oct16	A	3.5	12 04 03.75	+31 53 44.0	9.7	100
NGC 4096	2000Oct16	A	3.5	12 06 00.72	+47 28 38.2	8.8	100
NGC 4123 ^c	1983–1989	A,B	34	12 08 11.11	+02 52 42.0	25.3	45
NGC 4136	2000Oct16	A	3.5	12 09 17.70	+29 55 40.0	9.7	100
NGC 4254	1985–1989	A,B,BnA	139	12 18 49.33	+14 25 08.9	16.8	50
NGC 4298	2000Oct16	A	3.5	12 21 32.75	+14 36 22.9	16.8	100
NGC 4535 ^c	1985May19	B	7	12 34 20.28	+08 11 52.1	16.8	115
NGC 4605	2000Oct16	A	3.5	12 40 00.00	+61 36 29.0	4.0	100
NGC 4647	2000Oct16	A	3.5	12 43 32.31	+11 34 54.7	16.8	100
NGC 4900	1983Aug15	A	12	13 00 38.98	+02 29 57.4	17.3	108
NGC 5300	2000Oct16	A	3.5	13 48 15.90	+03 57 03.0	23.1	100
NGC 5690	2000Oct16	A	3.5	14 37 41.27	+02 17 28.2	28.8	100
NGC 5775	1984,1990	A	61	14 53 57.36	+03 32 42.2	26.7	38
NGC 5907 ^c	1984Dec08	A	4	15 15 49.12	+56 20 27.1	14.9	160
NGC 6207	2000Oct16	A	3.5	16 43 03.89	+36 49 56.8	17.4	127
NGC 6412	2000Oct16	A	3.5	17 29 37.51	+75 42 15.9	23.5	100
NGC 6643	2000Oct16	A	3.5	18 19 46.58	+74 34 07.9	25.5	100
NGC 7640	1989–1990	B	12	23 22 06.62	+40 50 43.40	8.6	77

^aObserved positions are quoted for undetected galaxies; images always were large enough to incorporate the currently accepted galaxy coordinates well within the fields of view.

^bDistances are taken from Tully 1988.

^cThe quoted position refers to the strongest detected source associated with the galaxy.

emission identified with the galaxy nucleus. Here, we report on a study of a subsample of H II nuclei in Sc galaxies from the Palomar bright galaxy sample, in which we test for the presence of weak AGNs and central black holes by searching for radio emission from the galaxy nuclei.

2. SAMPLE SELECTION AND OBSERVATIONS

In order to provide a uniform sample, we chose the 57 objects classified as Sc ($T = +5$) in the Ho et al. (1997a) catalog of H II galaxies. Due to the constraints of limited observing time, we selected a distance-limited sample of 41 of these galaxies lying within 30 Mpc. In this sample, 15 objects had 6-cm data

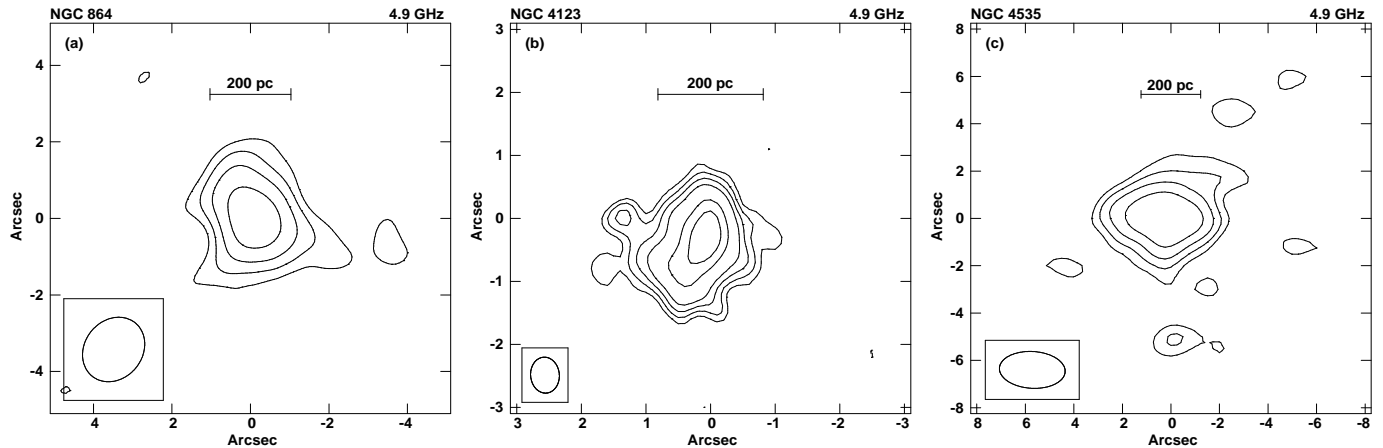


FIG. 1.— Images at 4.9 GHz of the three detected nuclear radio sources from the H II galaxy sample. All contour levels start at 3 times the rms noise in the image, and increase by factors of $\sqrt{2}$. Scale bars indicating linear sizes of 200 pc are indicated on all images. (a) NGC 864: rms noise of $49 \mu\text{Jy beam}^{-1}$, peak flux density of $0.55 \text{ mJy beam}^{-1}$, beam size $1''.77 \times 1''.48$ at PA = -35° . (b) NGC 4123: rms noise of $45 \mu\text{Jy beam}^{-1}$, peak flux density of $1.39 \text{ mJy beam}^{-1}$, beam size $0''.57 \times 0''.44$ at PA = 5° . (c) NGC 4535: rms noise of $115 \mu\text{Jy beam}^{-1}$, peak flux density of $1.66 \text{ mJy beam}^{-1}$, beam size $2''.71 \times 1''.55$ at PA = 87° .

at $\lesssim 1''$ resolution in the VLA archive, from observations made in the high-resolution **A** and **B** configurations, or the hybrid **BnA** configuration with a long north arm (see Thompson et al. 1980). Data for these objects were extracted from the archive. Twenty-five sample galaxies, as well as one galaxy at a distance slightly greater than 30 Mpc (IC 467), were observed by us on 16 October 2000, using the VLA **A** configuration. All new observations were centered at a frequency of 4.86 GHz, with a total bandwidth of 100 MHz in each of two circular polarizations. One galaxy that met our selection criteria, NGC 3430, was not observed because of the apparent presence of data in the VLA archive, but we later found that there were no usable archive data.

Approximately 3.5 minutes were spent integrating on each of the newly observed galaxies, providing a detection threshold about 2.2 times higher than for the Seyfert galaxies observed by Ho & Ulvestad (2001). For the archive data, total integration times ranged from a few minutes to more than two hours. Table 1 summarizes the new and archival observations of the galaxies, including the nominal positions for the galaxy nuclei that were used for imaging. For the seven detected galaxies (see Section 3), the listed positions are those of the peaks of the radio sources apparently associated with the galaxies. All images covered fields of at least $100''$ in both right ascension and declination, usually centered at the nominal galaxy positions at the times of the observations. In two galaxies, NGC 3666 and NGC 5907, the currently accepted positions for the galaxy nuclei are more than $15''$ from the original pointing positions, so the data for these sources were phase-shifted to the more accurate galaxy positions in order to center the images on the nuclei.

Processing of both new and archival data sets was similar, and was performed in the NRAO Astronomical Image Processing System (van Moorsel, Kemball, & Greisen 1996). The flux-density scales were set by observations of 3C 48 and 3C 286, using the scale of Baars et al. (1977), with slight adjustments for variability that have been found by VLA staff. A local calibrator was observed for each galaxy, in order to transfer the amplitude scale from the primary flux calibrators and to provide a local phase calibration, removing the effects of electronics and atmosphere. If more than one data set was available

from the archive for a given galaxy, each data set was calibrated individually and then combined. Bad data were identified and flagged, and deconvolution and imaging then was performed on the calibrated data sets. All data sets were imaged with “natural” weighting in the (u,v) plane in order to provide the best possible sensitivity. For data sets with excess noise or obvious stripes in the images, confusing sources were imaged and self-calibrated in order to reduce the noise level. The 1σ rms noise was $100 \mu\text{Jy beam}^{-1}$ for all the new observations, and varied depending on data quality and quantity, as well as array configuration for the archival data (see Table 1). Synthesized beam sizes were $0''.4$ – $0''.5$ for the new **A** configuration data, and $0''.4$ to as much as $2''$ for the archival data.

3. RESULTS

The range of resolutions and galaxy distances (typically 15–30 Mpc) provides linear resolutions in the range of 40 to 300 pc, sufficient to isolate the galaxy center from the rest of the galaxy. None of the 26 newly observed galaxies was detected, with a 5σ upper limit of $0.5 \text{ mJy beam}^{-1}$ for each. For the 15 galaxies whose archival data were analyzed, seven were detected: NGC 864, 1073, 3359, 3877, 4123, 4535, and 5907. The flux densities and powers of the detected galaxies are summarized in Table 2, while the positions of their radio peaks were given in Table 1.

The noise levels for the archival data often were lower than for the new data due to longer integration times, but only one of the detections was weaker than the upper limit for the new data. However, the archival galaxies often contain significant amounts of data from the larger **B** configuration, sensitive to more extended structures of lower surface brightness than for the new **A** configuration data. The beam area in the larger configuration typically is 10 times larger than the beam area in the smaller configuration; the respective beam diameters are $\sim 130 \text{ pc}$ and $\sim 40 \text{ pc}$ at the median galaxy distance of 17 Mpc. If the radio sources tend to be resolved on scales of 100–200 pc, an increased peak flux density would be seen in the lower resolution data, perhaps moving the galaxies above our detection threshold. This possibility is supported by the fact that the detected nuclear radio sources in three galaxies are partly resolved

TABLE 2
DETECTIONS OF H II GALAXIES

(1) Galaxy	(2) Peak (mJy beam ⁻¹)	(3) Total (mJy)	(4) Log ($P_{6,\text{peak}}$) (W Hz ⁻¹)	(5) Log ($P_{6,\text{total}}$) (W Hz ⁻¹)
NGC 864	0.5	1.3	19.42	19.79
NGC 1073 ^a	3.8	3.8	20.14	20.14
NGC 3359 ^a	0.4	0.4	19.25	19.25
NGC 3877 ^b	1.2	1.2	19.62	19.62
NGC 4123	1.6	6.6	20.09	20.71
NGC 4535	1.7	6.7	19.76	20.36
NGC 5907 ^{a,c}	1.7	2.4	19.65	19.80

^aThe detected radio source is not associated with the nucleus of the galaxy.

^bThe detected radio source is associated with SN 1998S.

^cThe source appears slightly smeared due to the finite bandwidth and the large distance from the field center.

by the VLA (see Section 4.1 for more details).

4. ORIGINS OF THE RADIO EMISSION

4.1. Locations of the Detected Radio Sources

In this section, we consider primarily the H II galaxies that were detected by the VLA. Only three of those galaxies have radio detections consistent with the positions of their nuclei as given in the NASA Extragalactic Database (NED) and confirmed with the measurements of Cotton, Condon, & Arbizani (1999). The three nuclear detections are in the galaxies

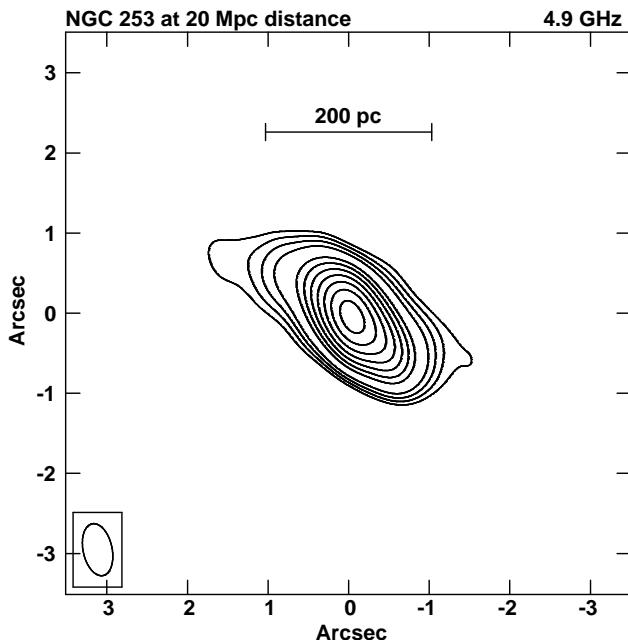


FIG. 2.— VLA image of NGC 253, from Ulvestad & Antonucci (1997), degraded in resolution and flux density to indicate its appearance viewed at a distance of 20 Mpc. Contours increase by $\sqrt{2}$ from a lowest level of $150 \mu\text{Jy beam}^{-1}$. At 20 Mpc distance, the beam size is $0''.66 \times 0''.36$ at PA = 12° , and the peak flux density is $8.22 \text{ mJy beam}^{-1}$.

NGC 864, NGC 4123, and NGC 4535. NGC 1073 has two

sources detected in the field, one associated with a background quasar identified by Colbert & Ptak (2002); the other detection may be associated with the galaxy, but is located approximately $30''$ from the nucleus at position angle 37° , and is not coincident with either of the intermediate-luminosity X-ray objects shown by Colbert & Ptak (2002). NGC 3359 has a detection about $9''.5$ south of the nucleus, and NGC 5907 has a detection nearly an arcminute away from the nucleus, possibly associated with the disk of the edge-on host galaxy. Finally, the only source detected in NGC 3877 is at the location of the Type II supernova SN 1998S, whose radio detection using the same data was reported previously by Van Dyk et al. (1999).

Figure 1 shows the radio images of the three nuclear radio sources found in our survey. All three are resolved and appear somewhat diffuse (as opposed to “jet-like”), with diameters of ~ 300 parsecs. This radio emission may be associated with starbursts, but the unresolved components of the core radio emission conceivably may be associated with AGNs. For these three nuclear radio sources, NGC 864 and NGC 4535 contain only data from the **B** configuration of the VLA, whereas NGC 4123 has data from both the **A** and **B** configurations. To test the effects of resolution on galaxy detectability, we have made images of NGC 4123 containing only the **A** configuration data and only the **B** configuration data. The peak flux density of the nuclear source is a factor of 3 higher in the **B** configuration image than in the **A** configuration image ($4.4 \text{ mJy beam}^{-1}$ vs. $1.4 \text{ mJy beam}^{-1}$), as expected from inspection of Figure 1. If the same ratio had held for NGC 864 and NGC 4535, NGC 864 would not have been detected in our short **A** configuration integrations, whereas NGC 4535 would have been marginally detected. Therefore, the generally higher sensitivity to extended structures in the archival galaxies accounts for at least some of the increased detection probability for these objects. In fact, it may be that a significant fraction of the galaxies that were not detected in the October 2000 observing run would have been detected using a more compact VLA configuration.

4.2. Radio Emission Associated with Star Formation

A young starburst typically can give rise to thermal radio emission from collections of H II regions or super star clusters, or to nonthermal radio emission from collections of supernova remnants. Such radio emission, with varying ratios of thermal

TABLE 3
SUPERNOVA RATES REQUIRED FOR RADIO EMISSION FROM H II GALAXIES

(1) Galaxy	(2) Galaxy Center		(4) Entire Galaxy	
	$\text{Log } (P_{20,\text{nucleus}})^{\text{a}}$ (W Hz ⁻¹)	ν_{SN} (yr ⁻¹)	$\text{Log } (P_{20,\text{galaxy}})^{\text{b}}$ (W Hz ⁻¹)	ν_{SN} (yr ⁻¹)
NGC 864	<19.94	<0.001	21.16	0.01
NGC 4123	20.96	0.008	21.23	0.02
NGC 4535	20.37	0.002	21.48	0.03

^aThe nuclear 20-cm radio powers are taken from Hummel et al. 1987.

^bThe galaxy 20-cm radio powers are derived from flux densities measured from the NRAO VLA Sky Survey Condon et al. 1998.

and nonthermal components, is observed in starburst galaxies such as NGC 253 (Antonucci & Ulvestad 1988; Ulvestad & Antonucci 1997; Johnson et al. 2001), M82 (Kronberg, Biermann, & Schwab 1985; Muxlow et al. 1994), Henize 2-10 (Kobulnicky & Johnson 1999; Beck, Turner & Gorjian 2001), and NGC 5253 (Turner, Beck, & Ho 2000; Gorjian, Turner, & Beck 2001), or in merger galaxies such as NGC 4038/9 (Neff & Ulvestad 2000). The three H II galaxies with nuclear radio detections that are shown in Figure 1 have radio sizes of a few hundred parsecs, indicating that any intense star formation must be confined to the near-nuclear regions of the galaxies.

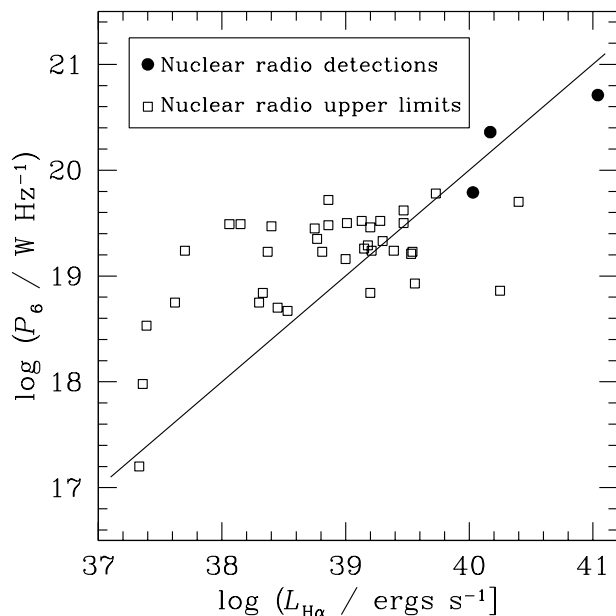


FIG. 3.— Plot of radio power vs. $H\alpha$ luminosity for 40 Sc galaxies with H II nuclei in the statistical sample. Radio detections and upper limits are distinguished by different symbols. The diagonal line is a prediction of thermal radio emission based on the $H\alpha$ luminosity, using P_6 (W Hz⁻¹) $\approx 10^{-20} L_{H\alpha}$ (ergs s⁻¹) (Filho et al. 2002).

The 4.9-GHz radio sizes of NGC 864, NGC 4123, and NGC 4535 are quite similar to the 500–600 pc nuclear starburst in the nearby Sc galaxy NGC 253 (Antonucci & Ulvestad 1988; Ulvestad & Antonucci 1997). NGC 253 has a total 5-GHz flux

density of 2.4 Jy integrated over the entire galaxy (Griffith et al. 1994). However, the flux density found by integrating over the central NGC 253 starburst in the 4.9-GHz image shown by Ulvestad & Antonucci (1997) is only 1.3 Jy, corresponding to a radio power of 9.6×10^{20} W Hz⁻¹. The three H II nuclei whose detections are reported here have radio powers ranging from a factor of 2 (for NGC 4123) to a factor of 15 (for NGC 864) lower than this central starburst in NGC 253. Thus, it is entirely possible that the detected H II galaxies harbor nuclear star formation somewhat weaker than that in NGC 253. Supporting this possibility, Figure 2 shows the 6-cm image of NGC 253 (Ulvestad & Antonucci 1997), as it would appear at a distance of 20 Mpc instead of at 2.5 Mpc, having the flux density reduced by a factor of 64, and angular resolution degraded by a factor of 8 in each dimension. The radio morphology of this degraded NGC 253 image looks similar to the H II galaxies in Figure 1, except that the respective peak and total flux densities are somewhat higher, at 8.2 mJy beam⁻¹ and 20 mJy.

The archival 6-cm data for NGC 864 and NGC 4535 were taken in the **B** configuration, and we also have measured a flux density from the **B** configuration 6-cm data for NGC 4123 (total flux density given in Table 2). Comparing the 6-cm values with the 20-cm **A** configuration flux densities (at similar angular resolution) published by Hummel et al. (1987) indicates that the resolved nuclear sources in NGC 4123 and NGC 4535 have respective two-point spectral indices (using $S_\nu \propto \nu^{+\alpha}$) of -0.51 and -0.02 ; due to its non-detection at 20 cm, the spectral index of NGC 864 is limited to a value greater than -0.27 . The relatively flat spectra of at least two of the objects may be indicative of radio emission dominated by optically thin thermal emission from star formation regions.

For a thermal radio source, both the hydrogen emission lines and the free-free radio emission are powered by ionizing photons from hot young stars. The radio power and $H\alpha$ luminosity are related by (Filho, Barthel, & Ho 2002)

$$P_6 \text{ (W Hz}^{-1}\text{)} \approx 10^{-20} L_{H\alpha} \text{ (ergs s}^{-1}\text{)}. \quad (1)$$

For all 40 H II galaxies observed in our distance-limited sample (those in Table 1 except for IC 467), Figure 3 plots the radio power against the $H\alpha$ luminosity given by Ho et al. (1997a)². This figure shows that three of the five galaxies with the highest

² As explained in Ho, Filippenko, & Sargent (2002), some of the $H\alpha$ luminosities published in Ho et al. (1997a) have been updated with more accurate values from the literature. These are listed in Ho et al. (2002).

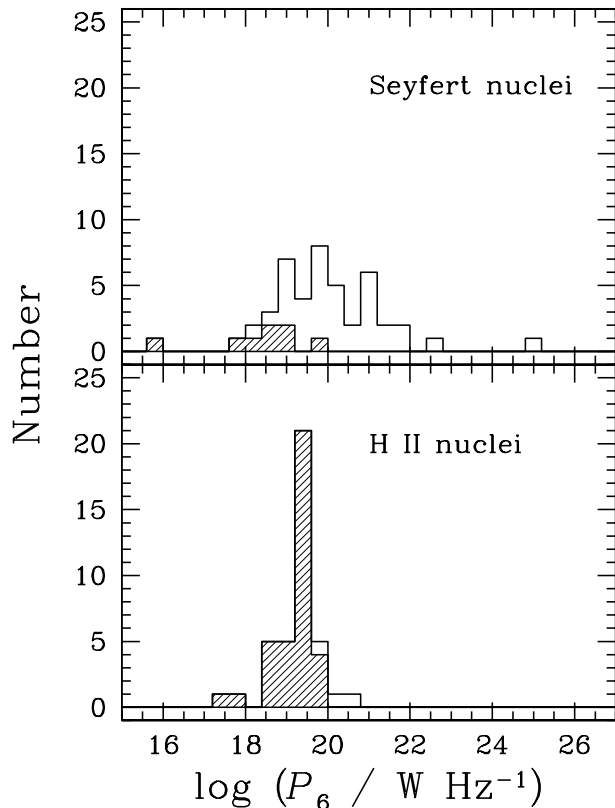


FIG. 4.— Histogram of radio powers of 40 Sc galaxies with H II nuclei within 30 Mpc, compared to Seyfert galaxies from the same Palomar galaxy sample. Powers for the Seyfert galaxies have been taken from Ulvestad & Ho (2001). Upper limits are shown hatched.

$H\alpha$ luminosities harbor detected nuclear radio sources. Furthermore, these three detected galaxies fall near the relation given by Equation 1, supporting the inference (from their spectra) that their radio emission has a significant thermal component. We note that the radio upper limits for some of the undetected galaxies actually are below the predictions based on the nuclear $H\alpha$ luminosity, with the largest discrepancy existing for NGC 3877. Since the $H\alpha$ luminosities were measured with a $2''$ by $4''$ aperture, it may be that nuclear thermal radio sources have been over-resolved by the higher resolution VLA imaging.

If the radio emission is thermal and related to starbursts, the inferred star formation rate also can be computed. Kennicutt (1998) gives the following formula for the star formation rate inferred from the $H\alpha$ luminosity, assuming a Salpeter mass function for 0.1– $100M_{\odot}$ and solar metallicity:

$$\text{SFR} (M_{\odot} \text{ yr}^{-1}) = 7.9 \times 10^{-42} L(H\alpha) (\text{ergs s}^{-1}). \quad (2)$$

For our three detected nuclei, the $H\alpha$ luminosities range from 10^{40} ergs s^{-1} to 10^{41} ergs s^{-1} so the inferred nuclear star formation rates that could account for the $H\alpha$ luminosity would be 0.08 – $0.8M_{\odot} \text{ yr}^{-1}$. Alternatively, using the formalism given by Condon (1992), the inferred star formation rates in stars above $5M_{\odot}$ are only 0.02 – $0.2M_{\odot} \text{ yr}^{-1}$.

Another possible result of a circumnuclear starburst would be a compact radio source with a steep spectrum, made up of complexes of supernova remnants that are unresolved by the VLA. Examples of these have been imaged at higher resolution by the Very Long Baseline Array (VLBA), in Arp 220 (Smith et al. 1998) and Mrk 231 (Taylor et al. 1999). The total radio powers can be used to estimate the associated supernova rates that would be required to account for the radio sources. We use

the formalism for an object whose total radio emission is dominated by cosmic rays accelerated in supernova remnants, but not identifiable with specific remnants. In this case, for a spectral index of -0.5 , Equation (18) of Condon (1992) becomes

$$\left(\frac{P_{20}}{10^{22} \text{ W Hz}^{-1}} \right) \sim 11 \left(\frac{\nu_{\text{SN}}}{\text{yr}^{-1}} \right). \quad (3)$$

For the nuclear radio sources, we can use the 20-cm radio emission found by Hummel et al. (1987) to estimate the nuclear supernova rates if the nuclear emission were entirely nonthermal (although the spectra appear thermal in two cases), and find values less than 0.01 yr^{-1} for all three galaxies. We also can compute the total supernova rates for the entire galaxies by using the galaxy flux densities determined from the NRAO VLA Sky Survey (Condon et al. 1998); this implies required supernova rates for the galaxies ranging from 0.01 yr^{-1} (NGC 864) to 0.03 yr^{-1} (NGC 4535). Results of the two different computations are summarized in Table 3. The star formation rates in stars above $5M_{\odot}$ (Condon 1992) required to account for the radio emission (presumed nonthermal) for the entire galaxies range from $\sim 0.3M_{\odot} \text{ yr}^{-1}$ to $\sim 1M_{\odot} \text{ yr}^{-1}$. These values are roughly an order of magnitude higher than those required for the nuclear sources, whether they are dominated by thermal or nonthermal emission. However, they are consistent with predictions for the entire galaxies that are based on the far-infrared fluxes measured by the *Infrared Astronomical Satellite* (Soifer et al. 1989; Moshir et al. 1990), converted to star formation rates using the formulation summarized by Kennicutt (1998).

4.3. Radio Emission Associated with Active Galactic Nuclei

The other possibility for the radio sources in the H II nuclei of Sc galaxies is that they have radio cores associated with AGNs and supermassive black holes. There has been considerable discussion in the literature about whether the core radio emission might be correlated with black hole masses in these cases (e.g., Franceschini, Vercellone, & Fabian 1998; Laor 2000). In fact, Ho (2002) contends that any correlation for weakly active galaxies is an indirect consequence of a more fundamental relationship between radio luminosity and optical bulge luminosity (or mass) as well as the established relationship between bulge luminosity and black hole mass.

Since Sc galaxies such as those in our H II sample generally have no well-defined bulges whose luminosities can be measured, and no known black holes, direct predictions of radio power cannot be made based on such properties. Instead, as a comparison, we have plotted a histogram of 6-cm nuclear radio powers for the 40 H II galaxies in our statistical sample in Figure 4, and compared the results to a similar plot for the statistical sample of 45 Seyfert nuclei (39 with galaxy types earlier than Sc) that was published by Ulvestad & Ho (2001). Application of the Gehan's Generalized Wilcoxon Test (Isobe & Feigelson 1990; LaValley, Isobe, & Feigelson 1992) indicates that the probability that the Seyferts and H II galaxies were drawn from the same parent population in radio luminosity is less than 10^{-4} . This result would be expected even if the H II galaxies contain AGNs, since they have faint or non-existent bulges, and there are no active galaxies with faint bulges that have high radio powers (Ho 2002).

In general, the radio sources in low-luminosity AGNs are quite compact. For the Seyferts from the Palomar sample, Ho & Ulvestad (2001) showed that about half the objects have diameters of ~ 100 pc or less. In the case of LINERs, Nagar et

al. (2000) demonstrated that those with flat radio spectra typically have AGN radio cores with diameters less than 25 pc, and Falcke et al. (2000) used the VLBA to show that these cores typically are parsec-scale or smaller. The radio peaks of NGC 864, NGC 4123, and NGC 4535, having size limits less than 50–150 pc, are consistent with the presence of AGNs but are not required to be black-hole powered. Instead, the trend of decreasing peak flux density with higher resolution seen in NGC 4123 (see Section 4.1) indicates that those peaks probably would be resolved if somewhat smaller spatial scales (longer baselines) were sampled. If so, AGNs are unlikely to contribute much to the currently unresolved radio emission. If there really are weak AGNs causing the most compact radio emission, they should be detectable with the VLBA, as are many other low-luminosity AGNs (Falcke et al. 2000; Nagar et al. 2002).

5. SUMMARY

We have searched for nuclear radio sources in a statistical sample of 40 Sc galaxies hosting H II nuclei, using imaging of new and archival VLA data at 6 cm. Only three such sources were detected, in galaxies among those with the largest H α luminosities in the sample. The radio powers and morphologies are consistent with the association of the detected radio sources with nuclear starbursts similar to that in NGC 253, rather than being caused by active galaxies powered by massive black holes. The ratio of radio power to H α luminosity is generally consistent with thermal radio emission from nuclear starbursts, and the detected central sources could produce such thermal

emission for star formation rates of only 0.08–0.8 M_{\odot} yr $^{-1}$. However, nonthermal emission from supernova remnants also could contribute to the detected nuclear sources, requiring supernova rates of well under 0.01 yr $^{-1}$ and star formation rates of $\sim 0.1 M_{\odot}$ yr $^{-1}$.

To the extent that radio cores are a common feature in low-luminosity AGNs, the nondetection of radio cores in H II nuclei strongly suggests that they intrinsically lack AGNs, and, by inference, massive black holes. This is not to say that late-type galaxies never host AGNs. Indeed, $\sim 15\%$ of the Seyfert nuclei and $\sim 10\%$ of all AGNs in the Palomar survey are hosted in galaxies with Hubble types Sc or later. In terms of AGN demographics, the present results imply that the existing statistics of AGNs in late-type galaxies based on optical searches (Ho et al. 1997b) are likely to be robust. There is not a large population of AGNs hidden among late-type galaxies that have H II spectra.

We thank the anonymous referee for extremely useful comments that helped clarify and focus the paper. This research has made use of the NASA/IPAC Extragalactic Database (NED) which is operated by the Jet Propulsion Laboratory, California Institute of Technology, under contract with the National Aeronautics and Space Administration. In addition, this research has made use of NASA's Astrophysics Data System Abstract Service. The work of L. C. H. is partly funded by NASA grants awarded by the Space Telescope Science Institute, which is operated by AURA, Inc., under NASA contract NAS5-26555.

REFERENCES

- Antonucci, R. R. J., & Ulvestad, J. S. 1988, *ApJ*, 330, L97
 Baars, J. W. M., Genzel, R., Pauliny-Toth, I. I. K., & Witzel, A. 1977, *A&A*, 61, 99
 Beck, S. C., Turner, J. L., & Gorjian, V. 2001, *AJ*, 122, 1365
 Colbert, E. J. M., & Ptak, A. F. 2002, *ApJS*, in press (astro-ph/0204002)
 Condon, J. J. 1992, *ARA&A*, 20, 575
 Condon, J. J., Cotton, W. D., Greisen, E. W., Yin, Q. F., Perley, R. A., Taylor, G. B., & Broderick, J. J. 1998, *AJ*, 115, 1693
 Cotton, W. D., Condon, J. J., & Arbizzani, E. 1999, *ApJS*, 125, 409
 Falcke, H., Nagar, N. M., Wilson, A. S., & Ulvestad, J. S. 2000, *ApJ*, 542, 197
 Ferrarese, L., & Merritt, D. 2000, *ApJ*, 539, L9
 Ferrarese, L., Pogge, R. W., Peterson, B. M., Merritt, D., Wandel, A., & Joseph, C. L. 2001, *ApJ*, 555, L79
 Filho, M. E., Barthel, P. D., & Ho, L. C. 2002, *ApJS*, in press (astro-ph/0205196)
 Franceschini, A., Vercellone, S., & Fabian, A. C. 1998, *MNRAS*, 297, 817
 Gebhardt, K., et al. 2000a, *ApJ*, 539, L13
 ——. 2000b, *ApJ*, 543, L5
 ——. 2001, *AJ*, 122, 2469
 Gorjian, V., Turner, J. L., & Beck, S. C. 2001, *ApJ*, 554, L29
 Griffith, M. R., Wright, A. E., Burke, B. F., & Ekers, R. D. 1994, *ApJS*, 90, 179
 Ho, L. C. 2002, *ApJ*, 564, 120
 Ho, L. C., Filippenko, A. V., & Sargent, W. L. W. 1995, *ApJS*, 98, 477
 ——. 1997a, *ApJS*, 112, 315
 ——. 1997b, *ApJ*, 487, 568
 ——. 2002, *ApJ*, submitted
 Ho, L. C., & Ulvestad, J. S. 2001, *ApJS*, 133, 77
 Hummel, E., van der Hulst, J. M., Keel, W. C., & Kennicutt, R. C., Jr. 1987, *A&AS*, 70, 517
 Isobe, T., & Feigelson, E. D. 1990, *BAAS*, 22, 917
 Johnson, K. E., Kobulnicky, H. A., Massey, P., & Conti, P. S. 2001, *ApJ*, 559, 864
 Kennicutt, R. C., Jr. 1998, *ARA&A*, 36, 189
 Kobulnicky, H. A., & Johnson, K. E. 1999, *ApJ*, 527, 154
 Kormendy, J., & Gebhardt, K. 2001, in 20th Texas Symposium on Relativistic Astrophysics, AIP Conf. Proceedings 586, ed. J. C. Wheeler & H. Martel (New York: American Institute of Physics), 363
 Kronberg, P. P., Biermann, P., & Schwab, F. R. 1985, *ApJ*, 291, 693
 Laor, A. 2000, *ApJ*, 543, L111
 LaValley, M., Isobe, T., & Feigelson, E. D. 1992, in ASP Conf. Ser. 25, *Astronomical Data Analysis Software and Systems I*, ed. D. M. Worrall, C. Biemesderfer & J. Barnes (San Francisco: ASP), 245
 Magorrian, J., et al. 1998, *AJ*, 115, 2285
 Merritt, D., Ferrarese, L., & Joseph, C. L. 2001, *Science*, 293, 1116
 Moshir, M., et al. 1990, *IRAS Faint Source Catalog, Version 2.0*
 Muxlow, T. W. B., Pedlar, A., Wilkinson, P. N., Axon, D. J., Sanders, E. M., & de Bruyn, A. G. 1994, *MNRAS*, 266, 455
 Nagar, N. M., Falcke, H., Wilson, A. S., & Ho, L. C. 2000, *ApJ*, 542, 186
 Nagar, N. M., Falcke, H., Wilson, A. S., & Ulvestad, J. S. 2002, *A&A*, in press (astro-ph/0207176)
 Neff, S. G., & Ulvestad, J. S. 2000, *AJ*, 120, 670
 Sandage, A. R., & Tammann, G. A. 1981, *A Revised Shapley-Ames Catalog of Bright Galaxies* (Washington, DC: Carnegie Inst. of Washington)
 Smith, H. E., Lonsdale, C. J., Lonsdale, C. J., & Diamond, P. J. 1998, *ApJ*, 493, L17
 Soifer, B. T., Boehmer, L., Neugebauer, G., & Sanders, D. B. 1989, *AJ*, 98, 766
 Taylor, G. B., Silver, C. S., Ulvestad, J. S., & Carilli, C. L. 1999, *ApJ*, 519, 185
 Thompson, A. R., Clark, B. G., Wade, C. M., & Napier, P. J. 1980, *ApJS*, 44, 151
 Tremaine, S., et al. 2002, *ApJ*, 574, 740
 Tully, R. B. 1988, *Nearby Galaxies Catalogue* (Cambridge: Cambridge Univ. Press)
 Turner, J. L., Beck, S. C., & Ho, P. T. P. 2000, *ApJ*, 532, L109
 Ulvestad, J. S., & Antonucci, R. R. J. 1997, *ApJ*, 488, 621
 Ulvestad, J. S., & Ho, L. C. 2001, *ApJ*, 558, 561
 Van Dyk, S. D., Lacey, C. K., Sramek, R. A., & Weiler, K. W. 1999, *IAUC* 7322
 van Moorsel, G., Kembell, A., & Greisen, E. 1996, in *Astronomical Data Analysis Software and Systems V*, ed. G. H. Jacoby & J. Barnes (San Francisco: ASP), 37